Climatic Change
https://doi.org/10.1007/s10584-018-2213-3

Evaluations of NASA NEX-GDDP data over Southeast Asia: present and future climates

Srivatsan V. Raghavan[1] **· Jina Hur**[1] **· Shie-Yui Liong**[1,2]

Received: 1 May 2017 / Accepted: 21 April 2018

Abstract This study evaluates the National Aeronautics Space Administration (NASA) Earth Exchange Global Daily Downscaled Projections (NEX-GDDP) dataset that provides statistically downscaled CMIP5 historical and future climate projections (precipitation and temperature), at high spatial (25 km) and temporal (daily) resolutions. The study is performed over Southeast Asia for the historical period 1976–2005 and compared against gridded observations on daily scales. Future climate change is assessed over the future time slices, 2020–2050 and 2070–2099, under two Representative Concentration Pathways (RCP) scenarios 4.5 and 8.5 with respect to 1976–2005. The future climate projections indicate that surface temperatures over Southeast Asia are likely to increase by more than 3.5 °C by the end of the century. As to precipitation, both the mean and extreme rainfall are likely to increase but the biases in the historical simulations could contribute to larger uncertainties in the estimates of rainfall projections. Findings of the study indicate that NEX-GDDP are in good agreement with observations over the historical period only on monthly scales and that they do not capture the observed statistics on daily scales which suggests that these data need a deeper scrutiny on daily scales, especially when used for impacts studies.

1 Introduction

Earth System Models (ESMs) and Global Climate Models (GCMs), representing physical processes in the atmosphere, ocean, cryosphere, and land surface, are the most advanced tools currently available for modeling the response of the global climate system to increasing radiative forcing at large temporal and spatial scales. The user community of such information, however, often desires high-resolution output, given climate change impacts are seen at regional/local scales and at finer regional-local scales than simulated by these ESMs. To this end, the need of such climate information is realized through "downscaling" as the simulation

✉ Jina Hur
tmshurj@nus.edu.sg

[1] Tropical Marine Science Institute, National University of Singapore, Singapore, Singapore

[2] Willis Towers Watson, London, UK

Published online: 24 May 2018

accuracies of these global scale models are poor (Giorgi 1990; IPCC 2007) due to their coarse resolutions. The most common downscaling methods are dynamical and statistical (empirical) methods. The dynamical method employs a higher-resolution regional limited area model, widely known as a Regional Climate Model (RCM), driven using ESM/GCM outputs. Past regional climate model experiments such as PRUDENCE (Christensen et al. 2006) and current initiatives such as the Coordinated Regional Downscaling Experiments (CORDEX) (Jacob et al. 2014; Shongwe et al. 2015) are examples of the dynamical approach. The statistical method establishes empirical relationships between large-scale climate variables and regional and local variables and is seen as a cost-effective approach in downscaling and have been applied in various projects that deal with delivering climate projections for end-users (Maraun and Widmann 2018; Bosshard et al. 2013; Hewitson and Crane 2006). A general review of downscaling methods has been performed by Trzaska and Schnarr (2014) who suggest that there is no single best downscaling approach and all these approaches depend on the desired spatial and temporal resolution of outputs and the climate characteristics of the region of interest.

Given that the Southeast Asian region is highly climate vulnerable, the region requires high-resolution climate information that could help the research community as well as policymakers. However, only few studies on climate modeling and projections exist over Southeast Asia. Siew et al. (2014) evaluated a suite of CMIP5 models over the Southeast Asian region and noted that though many models broadly simulated the Southeast Asian winter monsoon features, the spread of bias was very large across the models. Chotamonsak et al. (2011) performed regional climate simulations over Southeast Asia and reported that the model reproduced the spatial distribution of temperature reasonably well, but precipitation was simulated with lesser skill than temperature. Ho et al. (2011) used the RCM RegCM3 to assess future climate changes over Vietnam and reported an increase in the hot summer days and a decrease in number of colder nights as a consequence of global warming. The Southeast Asia Climate Analysis and Modelling (SEACAM) framework was initiated by the Centre for Climate Research Singapore (CCRS) in 2011 in collaboration with the UK Met Office Hadley Centre (MOHC) in an effort to enhance regional scientific cooperation and increase scientific capacity among climate researchers in the Southeast Asia region where a team from different Southeast Asian countries analyzed climate data from six 25-km resolution 150-year PRECIS Regional Climate Model experiments over Southeast Asia (SEACAM 2014). The CORDEX initiative for Southeast Asia has completed its phase I, led by the National University of Malaysia, and is currently planning for a second phase to generate high-resolution climate projections for the region.

In this paper, we evaluate the past and future climates over Southeast Asia using the National Aeronautics and Space Administration (NASA) Earth Exchange Global Daily Downscaled Projections (NEX-GDDP) dataset which have been constructed at high spatial (25 km) and temporal (daily) resolutions which have been cited to be a promising source of climate projections at regional and local scales (Bao and Wen 2017). This study assumes significance given Southeast Asia is a highly climate vulnerable region where more research remains to be conducted on both climate modeling and impact studies. Developing countries in this region need robust scientific and technical expertise and good climate data to prepare for climate adaptation. Given that techniques such as dynamical downscaling are time and resources consuming, an easier option for these developing countries is to make use of data such as the NEX-GDDP to both have a first-cut understanding of plausible changes for their region and to apply them for impact studies.

In this context, we performed some initial evaluations on the NEX-GDDP data (temperature and precipitation) over the historical climate of Southeast Asia and assessed the possible future climate change over this region, under two of the Representative Concentration Pathway (RCP) scenarios, 4.5 and 8.5. In this exercise, we investigated how good the NEX-GDDP high-resolution data (spatial and temporal) are for climate studies on both monthly and daily time scales, while also assessing possible future climate changes over Southeast Asia. The paper is organized as follows: Sect. 2 provides an overview of the different data used and the methodology undertaken for data analyses, Sect. 3 illustrates the results of the assessment of the NEX-GDDP data over the baseline period, Sect. 4 assesses climate changes in the future, and Sect. 5 summarizes the discussions and draws some conclusions from this study.

2 Data

2.1 NASA NEX-GDDP

The National Aeronautics and Space Administration (NASA) Earth Exchange Global Daily Downscaled Projections (NEX-GDDP) dataset contains downscaled climate scenarios derived from the GCM simulations of the Coupled Model Intercomparison Project Phase 5 (CMIP5) and across two RCP emissions scenarios, 4.5 and 8.5. The spatial resolution of the dataset is 0.25° (~25 km × 25 km). These datasets provide a set of global, high-resolution, bias-corrected climate change projections that can be used to evaluate climate change impacts on finer scales. Each of the climate projections includes maximum and minimum temperatures and precipitation for the periods from 1950 through 2005 (retrospective run) and from 2006 to 2099 (prospective run) on a daily scale. A documentation is available at https://cds.nccs.nasa.gov/wp-content/uploads/2015/06/NEX-GDDP_Tech_Note_v1_08June2015.pdf. In this paper, we chose a subset of five models at random, with no specific ranking. These models are shown in Table 1. The downscaled data of these GCMs were downloaded from the NASA data portal at ftp://ftp.nccs.nasa.gov/.

2.2 Observational data

2.2.1 CRU (Climatic Research Unit data)

The Climatic Research Unit (CRU) precipitation and surface temperature (land only) datasets, CRU Time-Series (TS) Version 3.21 (Harris et al. 2014), have been used for most of the validations (on a monthly scale) that account for the precipitation over land areas. This dataset

Table 1 List of GCMs used in the study

No.	CMIP5 model	Resolution	Reference
1	CNRM-CM5	1.4°× 1.4°	Voldorie et al. (2013)
2	IPSL-CM5A-LR	1.8°× 3.75°	Dufresne et al. (2013)
3	NIES-MIROC5	1.4°× 1.4°	Watanabe et al. (2010)
4	MPI-ESM-MR	1.8°× 1.8°	Giorgetta et al. (2013)
5	MRI-CGCM3	1.12° × 1.12°	Yukimoto et al. (2012)

contains monthly values of global precipitation and temperature that spans the period 1901–2014, at a 0.5° spatial resolution.

2.2.2 SCU (Santa Clara University data)

This dataset contains daily precipitation and temperatures over the globe, spanning the period 1951–2008, at a 0.5° spatial resolution. The original dataset has been described by Adam and Lettenmaier (2003) and subsequently updated by Maurer et al. (2009). We refer to this dataset as "SCU," and these data are used in this study for those validations performed on a daily temporal scale. The data can be obtained at http://hydro.engr.scu.edu/files/gridded_obs/global_1950-2008/.

2.3 Methodology

The ensemble mean of the NEX-GDDP data were calculated using simple composite averages and were compared against CRU and SCU data. For comparison, CRU (50 km) and SCU (50 km) were resized to the same grid as the NEX-GDDP (25 km) using a bilinear interpolation which is an extension of linear interpolation on a rectilinear 2D grid as this resizing process does not generate any new information. The performance of the NEX-GDDP data was evaluated at multiple time scales such as annual, seasonal, and daily. For the spatial maps of climatological annual mean values, the surface temperature and precipitation were averaged over the baseline (1976–2005) and over the future periods (2020–2050, 2070–2099) at each grid point of the domain. For spatial maps of future climate change, regions where all models show the same change signal are shown by stippling. To investigate temporal variations, the annual mean values were area-averaged for all land-only points over Southeast Asia and the linear trend was computed during the period considered. The trend significance was calculated using the non-parametric Mann-Kendall test (Mann 1945; Kendall 1975) which is a statistical test for monotonic trends of the studied variable over time (Hirsch et al. 1982). To explore monthly patterns of precipitation, the time-latitude diagram, namely, Hovmoller, was plotted on the basis of the 1976–2005 climatological monthly mean, meridionally averaged for all land-only points over longitudes from 90° E to 140° E, centered at 104° E. Given that Southeast Asia is affected by seasonal monsoons and intra-monsoon periods, a seasonal evaluation was performed using the Taylor diagram. To investigate extreme events, both 1-day maximum value and box plot of the 90th percentile were computed at each domain grid point and then area-averaged over all land-only points over Southeast Asia. The box plot represents the minimum, lower quartile, median, higher quartile, and maximum values of the ensemble mean. In addition, the probability distribution functions (PDFs) were calculated for four major cities in Southeast Asia, Ho Chi Minh City, Manila, Jakarta, and Bangkok, by extracting the nearest grid point to the city coordinates from the NEX-GDDP data.

3 Results and discussions

3.1 Evaluations of the NEX-GDDP data over the baseline climate

The spatial distributions of the climatological (1976–2005) annual mean surface temperature over Southeast Asia is shown in Fig. 1. The NEX-GDDP distributions agree well against the

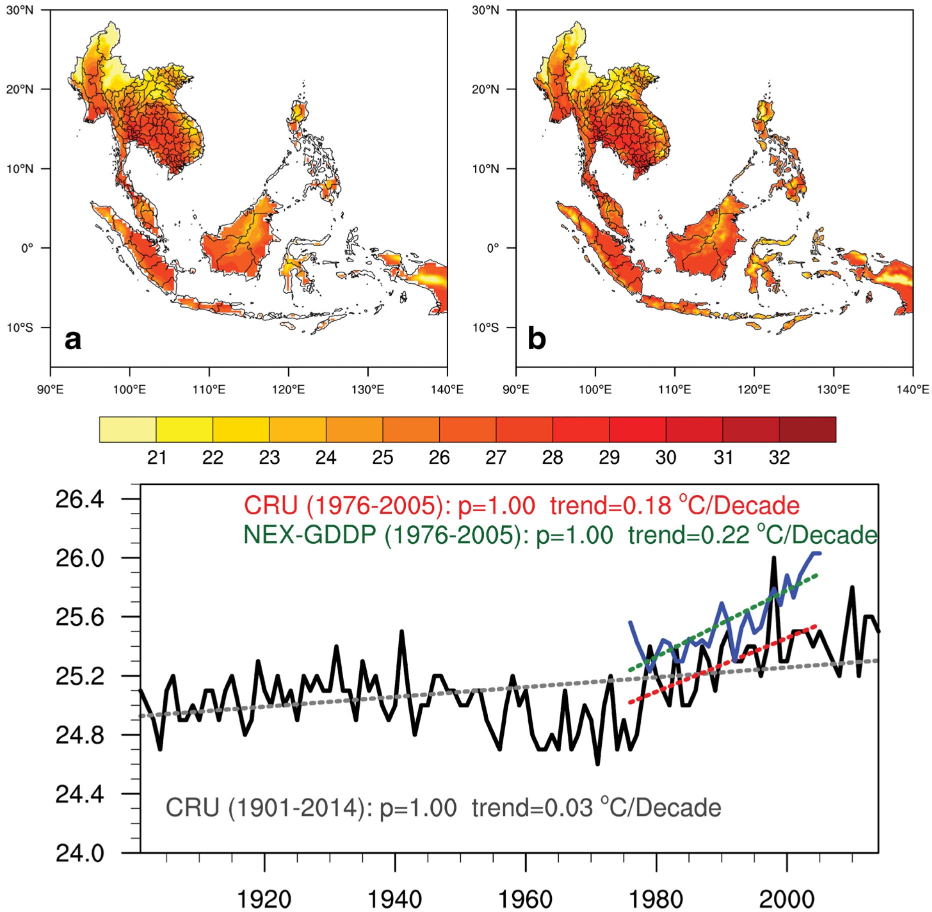

Fig. 1 (Top) spatial distribution of annual mean temperature, 1976–2005: **a** CRU and **b** NEX-GDDP. (Bottom) time series (°C) and trends (°C/decade); CRU (black) NEX-GDDP (blue)

CRU observations over almost all areas of the sub-continent. The relatively lower temperatures over the mountains are well-defined over western Sumatra, Java, and other islands of Indonesia including Borneo, Malay Peninsula, and over some highland regions of Vietnam as seen in the NEX-GDDP. CRU observations do not show these features in great detail possibly due to both lack of gauges at those remote sites and its spatial resolution (~ 50 km). Figure 1 shows the trend in the annual mean temperatures during the baseline period, 1976–2005. Though the comparison is performed for the baseline period, the time series of CRU, from 1901 onwards until 2014, is used to assess trends over the past century. The steady increases in the mean surface temperatures since 1976 are clearly seen in CRU. Though NEX-GDDP is in agreement with this increasing trend, the magnitudes of temperatures (0.22 °C increase per decade) are higher than CRU (0.18 °C increase per decade). These trends are statistically significant with a high confidence level (1.0 probability). It is also noticeable that the warmer tendency over the baseline period (1976–2005) is higher than one over the last hundred years (1901–2014), inferring that the effects of global warming have been rather significant.

Figure 2 shows the spatial distributions of the climatological (1976–2005) annual mean precipitation over Southeast Asia. In CRU, the heavy annual precipitation larger than 10 mm/day occurs in Borneo and mountainous areas over Sumatra (Indonesia) whereas scarce and light rains are seen over inland plains of Thailand. CRU does not represent detailed rainfall patterns over the Philippine archipelago characterized by complex climate types probably due to deficiency in gauge networks. The trends in rainfall suggest that the average (land points only) rainfall over Southeast Asia has been increasing since 1901, as seen in the CRU observations. However, CRU observations indicate an increase during the baseline period 1976–2005, of about 0.12 mm per decade, while NEX-GDDP shows a relatively mild increase of about 0.03 mm per decade. As in the case of temperature, the upward trends of precipitation over the recent period is more evident than the tendency of 0.02 mm per decade over the last

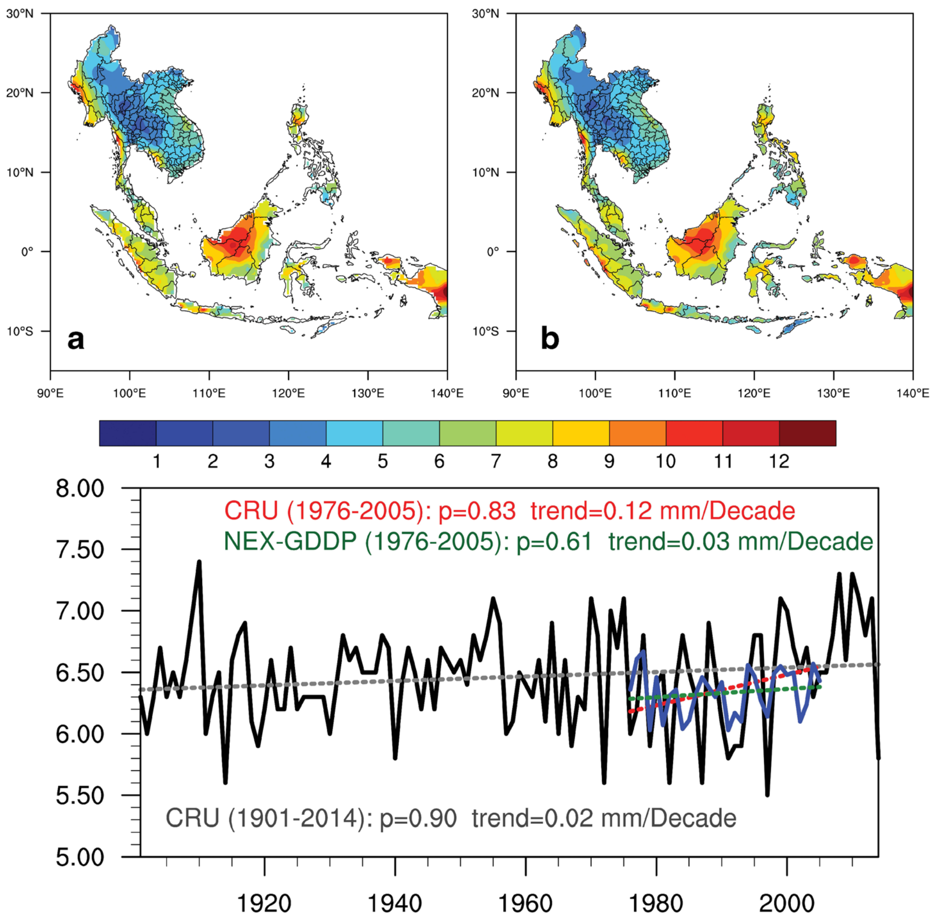

Fig. 2 (Top) spatial distribution of annual mean precipitation (mm/day) 1976–2005; **a** CRU and **b** NEX-GDDP (bottom). Time series (mm/day) and trends (mm/decade); CRU (black) NEX-GDDP (blue)

hundred years. Wetter tendencies of both data in annual mean precipitation are not statistically significant because the probabilities are 0.83 and 0.61, for CRU and NEX-GDDP, respectively.

It is also important to evaluate the performance of NEX-GDDP in simulating monthly rainfall variations (annual cycle) over Southeast Asia where northeast and southwest monsoons are dominant climatic features. This is shown using a Hovmoller diagram, seen in Fig. 3. The figure shows the climatological (1976–2005) annual cycle of rainfall over Southeast Asia, for CRU, and for the NEX-GDDP data. CRU shows a clear temporal evolution of monthly rainfall. The intense rainfall located in the equatorial region during the boreal winter period can be seen moving northward during summertime. NEX-GDDP reproduces the observed pattern and is in good agreement against CRU except some marginal differences in the rainfall magnitudes over some latitudes and during some months. In a quantitative evaluation of the NEX-GDDP, the Taylor diagram (Fig. 4) provides a concise statistical summary of how well the climate variables match observations in terms of correlation, root-mean-square difference, and the ratio of their variances (Taylor 2001). The figure shows all the five GCMs considered in this study and their ensemble average (compared against CRU) on both the annual and the seasonal scales. The diagram on the left compares the surface temperatures against the reference data, CRU, shown as “REF.” This figure suggests a good agreement of the global models against CRU with the high correlations of the individual five GCMs and their ensemble ranging between 0.85 and 0.96, though there is a spread among the different ensemble members in different time scales (annual and seasonal). Most of the models also exhibit a lower root mean squared error, except IPSL-CM5A-LR which shows outliers. MRI-CGCM3 is clustered during all time scales while the largest spreads are seen for CNRM-CM5, MIROC5, and MPI-ESM-MR. For the ensemble average, only the annual and the JJA (June–July–August) seasons are in close agreement with CRU. For precipitation, there is a large spread among the different GCMs and their ensemble. Among the five different global models, only CNRM-CM5 compares well against CRU during all time scales except the months of September through to November (SON). The figure shows the other models with lower spatial

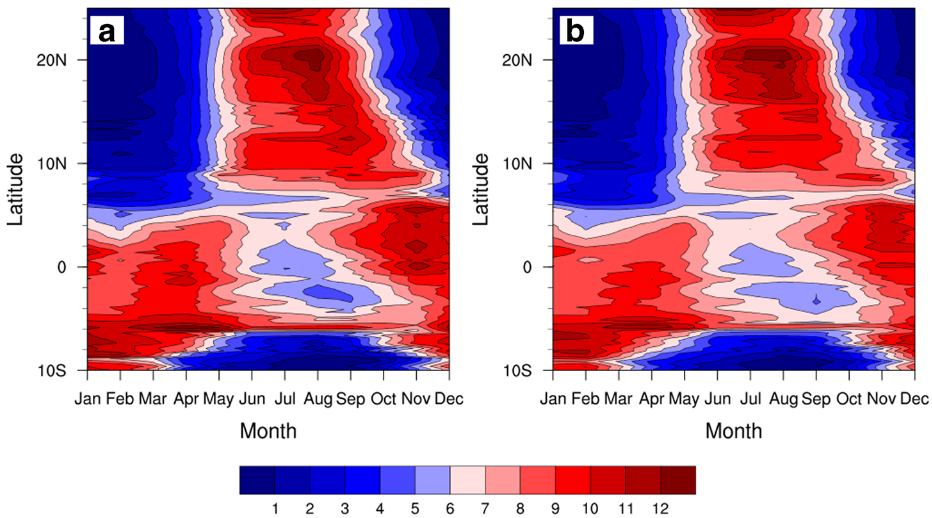

Fig. 3 Hovmoller diagram: annual cycle of rainfall climatology (mm/day) 1976–2005; **a** CRU and **b** NEX-GDDP

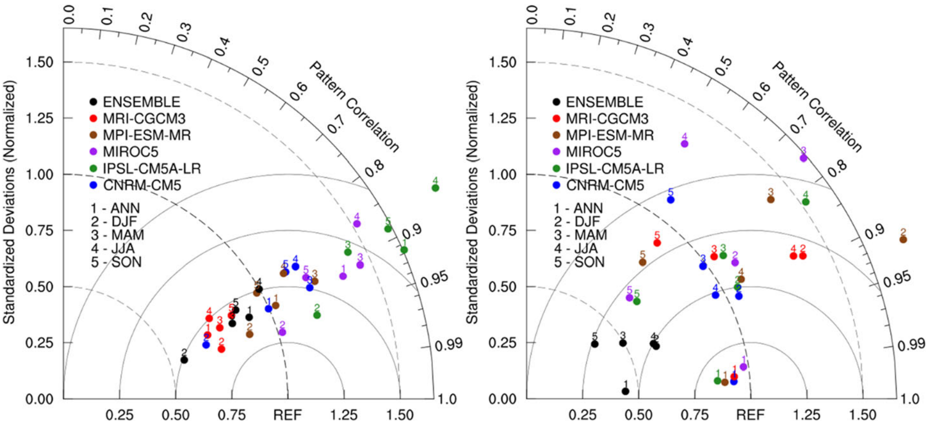

Fig. 4 Taylor diagram: (left) temperature, (right) precipitation, 1976–2005

correlations and higher root mean squared errors and standard deviations. The ensemble, however, does not show a good comparison against CRU, during all time scales.

3.2 Assessments of the future climate projections under the RCP scenarios

Figure 5 shows the past and future trends in the annual mean temperatures and precipitation of the NEX-GDDP ensemble compared to observations. The red and blue lines indicate the ensemble averages under each of the scenarios (RCP8.5 and RCP4.5), respectively. The annual mean temperature gradually increases over the whole period, but its trend is more pronounced under RCP8.5. This is seen through the trajectories of the future temperature that shows a wider range of increase under the RCP8.5 scenario compared to RCP4.5. For the period 2070–2090 (2020–2050), a warming decadal trend of RCP8.5 is 0.46 °C (0.34) per decade greater than RCP4.5 with an average trend of 0.07 °C (0.23) per decade. For precipitation, the magnitudes in the inter-annual variability is underestimated by NEX-GDDP, compared to CRU observations. Though a marginal increasing trend in rainfall is seen during the period 2020–2050, no clear trends can be seen during the last 30 years of the twenty-first century. Quantitatively, annual mean precipitation shows an increasing trend of 0.05 mm (0.04) per decade and 0.12 mm (0.17) per decade for RCP4.5 and 8.5 scenarios, respectively, over the period 2070–2099 (2020–2050). This suggests that the global warming does not result in a proportional increase in the mean state of precipitation. We also assessed the future changes in climate extremes. To compare the past and future trends on the daily extreme values in temperatures and rainfall, the daily observations SCU are used as reference against NEX-GDDP (Fig. 6). It is seen that the 1-day maximum temperature time series during the historical period underestimates observations, but the future trajectories are similar to that seen in Fig. 7. However, for rainfall, NEX-GDDP severely underestimates the observations during the historical period. This suggests that despite being bias corrected, NEX-GDDP does not compare well against observations at daily scales (higher temporal resolutions).

We evaluated the difference between the RCP scenarios and the historical simulations to project the change in daily extreme values. Although the change on the annual mean precipitation does not have any significant trends regardless of emission forcing, the 1-day maximum precipitation has an apparent increasing tendency over time. This demonstrates that

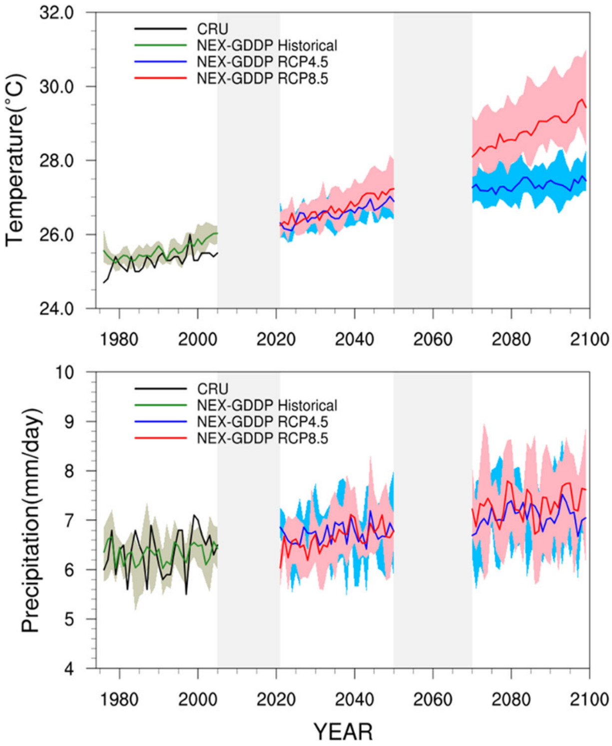

Fig. 5 Time series of annual mean temperature (°C) (top) and precipitation (mm/day) (bottom); CRU (black), historical (green), RCP4.5 (blue), and RCP8.5 (red). Future periods: 2020–2050 and 2070–2099 (white vertical patches show periods not considered in the study)

no trend in mean state does not necessarily mean no detectable patterns or trends of intense events and that higher emission concentrations can lead to more severe changes in both temperature and precipitation over Southeast Asia. The future trajectories indicate that while there are no significant differences in the trends between RCP4.5 and 8.5 scenarios during 2020–2050, RCP8.5 indicates a strong increase in the daily rainfall amounts towards the end of the century.

Figure 7 assesses the future change in the temperatures relative to the historical baseline period 1976–2005. Under both RCP scenarios, NEX-GDDP indicates increases of about 0.8–1.4 °C in the surface temperatures over the land areas of Southeast Asia during 2020–2050. Some regions over Myanmar and Thailand show similar magnitudes of changes under both RCP4.5 and 8.5. The increases in temperatures become more pronounced during 2070–2099 with RCP4.5 suggesting a maximum of 2 °C increases in many parts of the sub-continent. The RCP8.5 scenario shows increases of 3.5 °C and higher over almost all areas of Southeast Asia by the end of the century. Future changes in precipitation are assessed in Fig. 8. The NEX-GDDP change suggests that precipitation is on the increase (during 2020–2050) over most of the Southeast Asian land mass, except over some southern islands of Indonesia. It is also notable that the increases are pronounced under RCP4.5 than under RCP8.5, especially over the maritime continent during the 2020–2050 period. The precipitation response towards the end of the century indicates similar magnitudes of increases under both scenarios. However, notably, RCP8.5 simulates higher increases over the northern regions of Southeast Asia

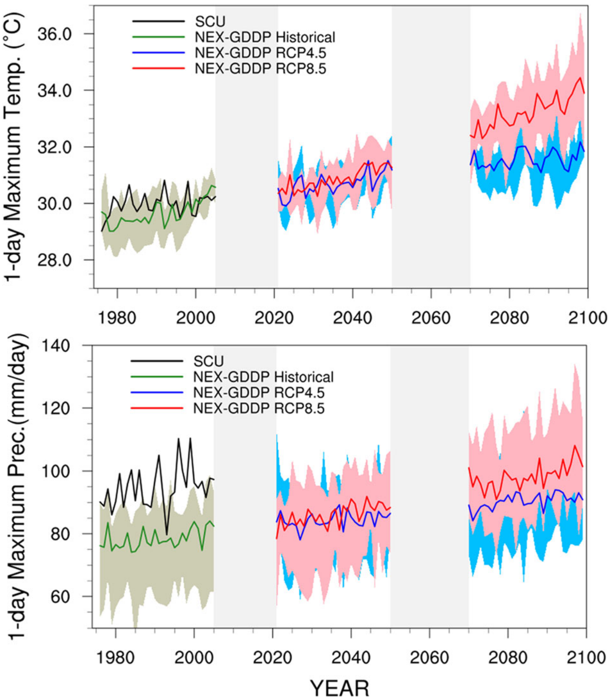

Fig. 6 Time series of 1-day maximum temperature (°C) and 1-day maximum precipitation (mm/day) in a year. Historical (green), RCP4.5 (blue), and RCP8.5 (red). Future periods: 2020–2050 and 2070–2099

comprising Vietnam, Cambodia, Lao P.D.R., and some areas of Myanmar. Figure 9 compares the 90th percentiles of the daily temperatures and rainfall against the SCU daily observations and provides their responses in the future climate. Over the baseline period, the historical NEX-GDDP simulates temperatures close to observations but strongly underestimates rainfall, as seen earlier. Daily maximum temperatures of more than 30 °C could be expected during the end of the century, under RCP8.5. This suggests that anomalously warm days in the current climate could probably be more common in the future. But it is cautioned here that this maximum temperature value of about 30 °C is the average of all land points over Southeast Asia, and hence, different regions and cities (at local scales) could have higher values. This is discussed further in Fig. 10. For rainfall, it can be seen clearly that the maximum daily rainfall is likely to increase strongly under RCP8.5 (a nearly 3 mm/per day increase relative to historical rainfall). However, given the underestimated magnitudes in the historical simulations, the actual increases could be far more than what is represented. These results, once again, suggest that the extreme values of rainfall are subject to high scrutiny when NEX-GDDP could be applied for impact studies or in policymaking. By the end of the twenty-first century, the 90th percentile precipitation under the RCP8.5 projection is likely to be 2.5 mm/day higher than in the baseline climate. The highest 90th percentile precipitation is seen under RCP8.5, followed by RCP4.5 and historical. This also suggests that the 90th percentile precipitation increases with increases in temperatures.

Though assessments at the regional scale are not indicative of changes at the local (city) scales, we attempt to analyze the changes in future temperatures and rainfall in four major

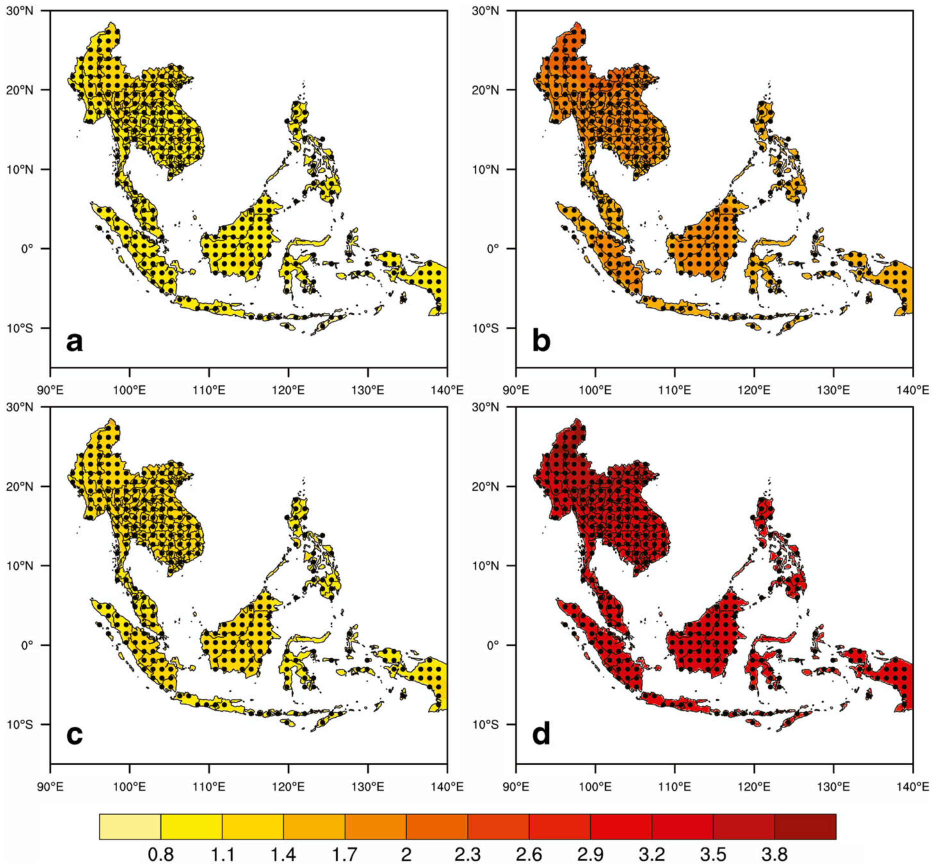

Fig. 7 Change in annual mean temperature (°C) relative to 1976–2005 RCP 4.5: **a** 2020–2050, **b** 2070–2099 RCP 8.5, **c** 2020–2050, **d** 2070–2099

cities in Southeast Asia, Ho Chi Minh City, Manila, Jakarta, and Bangkok. These cities are vulnerable to flooding, and hence, it is imperative to understand the magnitude of changes, especially in rainfall, that these cities may encounter in the future. Figure 10 shows the PDFs of NEX-GDDP data compared over historical and future time periods, for both temperature and rainfall. PDFs are generally regarded as a good indicator to measure the level of changes in both the mean state (e.g., central location) and the variance (e.g., dispersion) of the daily values. The PDFs of temperature clearly show the change in mean temperatures over the future, under the two RCP scenarios. It is evident that RCP8.5 indicates the largest change. It is also seen that extreme temperatures over these cities could be as high as 36 °C (Ho Chi Minh city) or higher (Bangkok). In the case of precipitation, except Jakarta, the PDFs fit a gamma distribution that shows light rain occurring more often than heavy ones. The distribution in the future projections does not show any significant differences against the historical climate but is altered in the lower and upper tail bounds. This is suggestive that the increase in greenhouse gas concentrations are likely to cause increases in downpour. NEX-GDDP fails to capture the observed distributions of the high-intensity rainfall in almost all cities and underestimates the rainfall magnitudes. This can be seen clearly in the inset diagrams of rainfall in Fig. 10. NEX-GDDP also fails to capture the frequencies of dry days when compared to SCU observations.

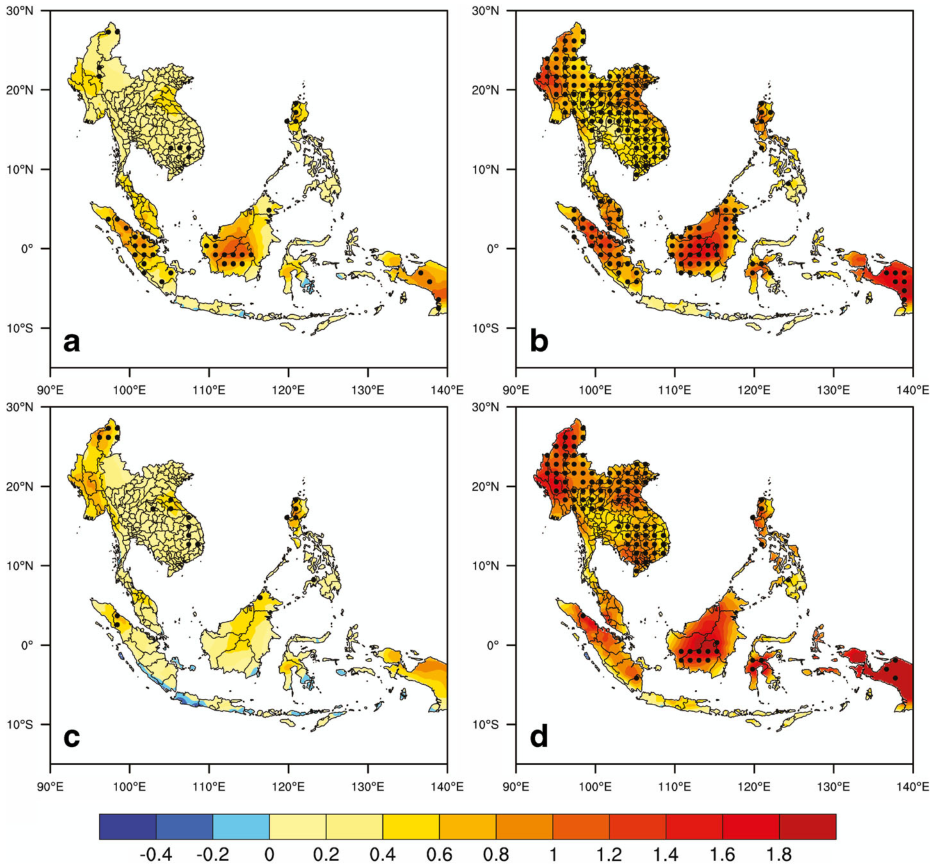

Fig. 8 Change in annual mean precipitation (mm/day) relative to 1976–2005 RCP 4.5: **a** 2020–2050, **b** 2070–2099 RCP 8.5, **c** 2020–2050, **d** 2070–2099

Overall, NEX-GDDP suggests an increase in light rainfall (2–10 mm/day) but no clear signal can be seen in the extremes, except over Manila where rain days more than 40 mm/day show a marginal increase. There is a tendency of the models to overestimate light rain and to underestimate heavy events. Yet again, the underestimation of historical magnitudes poses

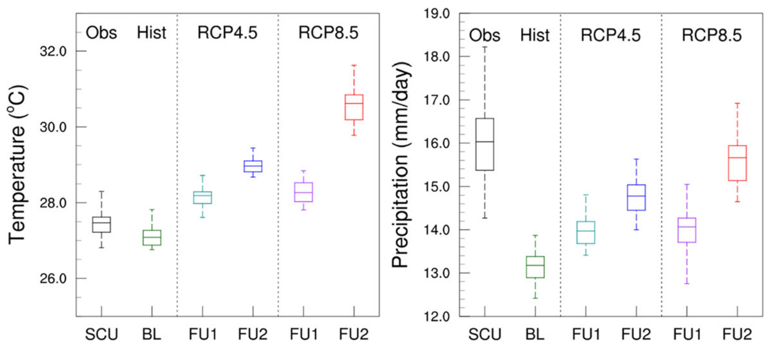

Fig. 9 Box plots of 90th percentile temperature (°C) and precipitation (mm/day) from Historical and Future. BL: baseline (1976–2005), FU1: 2020–2050, FU2: 2070–2099

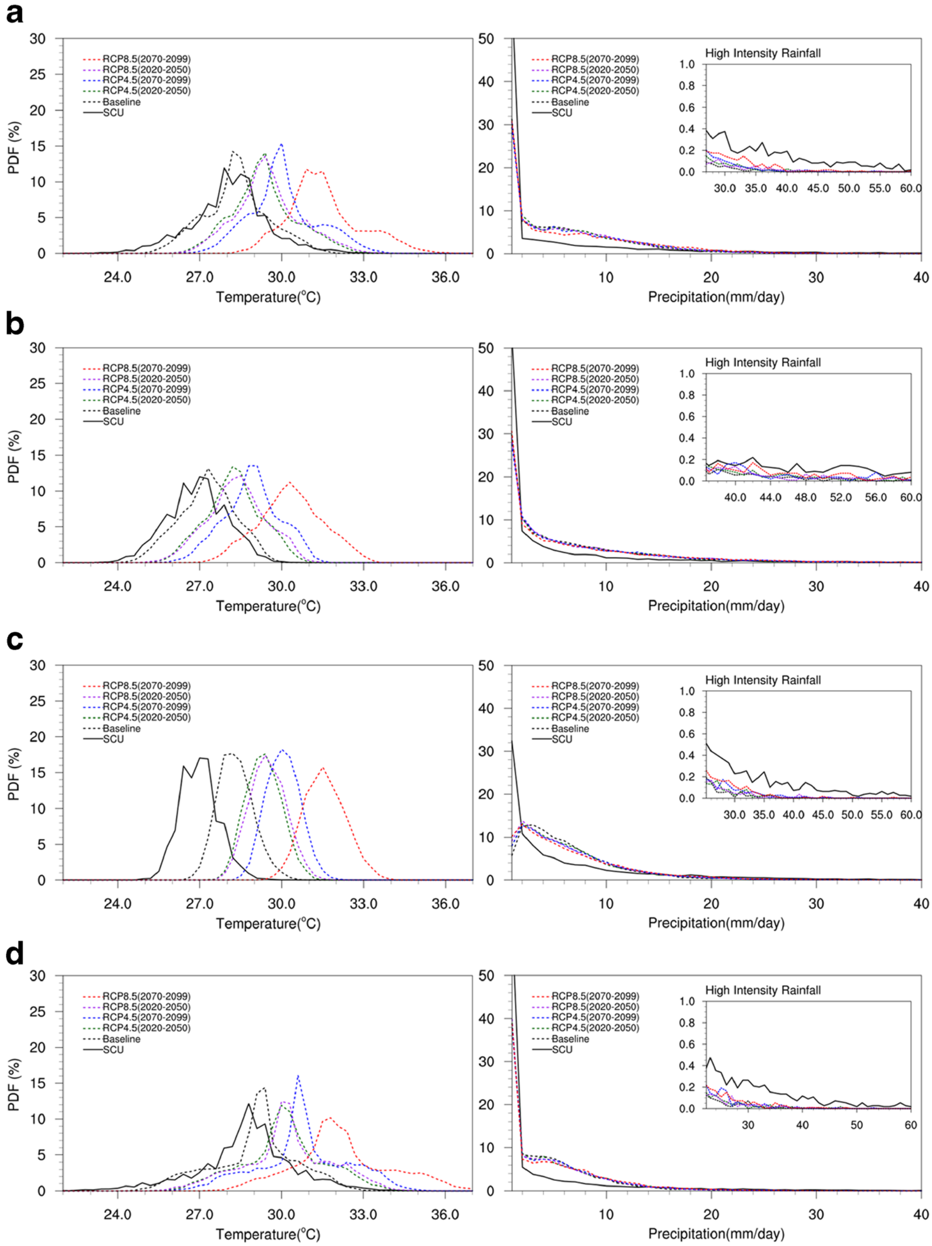

Fig. 10 Probability distribution functions: temperature and precipitation (Historical vs Future). **a** Ho Chi Minh city, **b** Manila, **c** Jakarta, **d** Bangkok

large uncertainties to the future changes in extremes and needs to be better quantified. In comparison between the scenarios, RCP8.5 has a thicker tail over all cities compared to RCP4.5 and historical, indicating that the cities are vulnerable to extreme rainfall events. It can also be concluded that the 1-day maximum (Fig. 8) and 90th percentile precipitations consistently project a warmer climate that induces enhancement of heavy rainfall. While temperature monotonically increases along with increases in greenhouse gas concentrations, precipitation does not seem to have a simple response to global warming.

These analyses reveal that NEX-GDDP performs better on monthly time scales than on daily time scales. To overcome both coarse resolution grids and locally biased statistical characteristics of ESM/GCM outputs, the Bias-Corrected Spatial Disaggregation (BCSD) method was used as a statistical downscaling algorithm in generating NEX-GDDP datasets (Thrasher et al. 2012). As a common feature of statistical downscaling methods, the algorithm is highly dependent on historical climate records because it is based on the comparison between the ESM/GCM outputs and the corresponding observations over a common period. For downscaling the near-surface meteorological variables, the Global Meteorological Forcing Dataset (GMFD) was employed as the observational climate data. In the process of generating GMFD, the daily precipitation was corrected using gauge-based CRU data and then temporally downscaled to a 3-hourly time step using the real-time Tropical Rainfall Measuring Mission (TRMM) products (Sheffield et al. 2006). It was also pointed out that these data can be biased due to several reasons: (1) the correction is focused on the rain day statistics rather than the fine-scale features of the historical record (e.g., storm events), (2) the ground-based data (e.g., CRU monthly data) cannot reflect detailed orographic effects due to an uneven distribution/lack of gauges at remote locations, and (3) the real-time TRMM dataset also contain biases at sub-daily scales (Sheffield et al. 2006). A recent research (Hur et al. 2017) also insisted that satellite-borne precipitation was unable to capture heavy rainfall at daily- and sub-daily scales over Southeast Asia because of sampling errors. Therefore, it is likely that uncertainties in the NEX-GDDP data, especially at daily scales, may be inherited from inaccuracy and quality of historical records/meteorological observations. Nevertheless, further scrutiny is advised when using these data at daily scales, for climate change assessments and impacts research.

4 Summary and conclusions

An evaluation of the historical (1976–2005) and plausible future (2020–2050, 2070–2099) changes in both temperature and precipitation in Southeast Asia was performed using the NEX-GDDP data. Overall, NEX-GDDP data represents well the mean states of temperature and precipitation on a monthly scale but daily scale data show limitations. On the basis of projections, the annual mean temperatures over Southeast Asia under the RCP4.5 and 8.5 scenarios are expected to increase by about 1.8 and 3.2 °C, respectively, with significant warming trends by the end of the century. The annual mean precipitation is also anticipated to increase by about 0.8 and 1.0 mm/day under RCP4.5 and 8.5 scenarios. According to the analysis of extreme events, the results reveal that increases in GHG concentrations might lead to enhancement of heat waves and intense rainfall. This suggests that Southeast Asia may become more prone to unusual weather events and uncertain precipitation. Despite bias-corrected data, NEX-GDDP underestimates observations at a daily scale in terms of 1-day maximum, 90th percentile rainfalls, and tail boundaries in PDF. This might result in a lot of uncertainties in interpreting the future plausible changes. Especially, these results demonstrate that the extreme values of precipitation are subject to high scrutiny when NEX-GDDP data could be applied for further impact studies or in policymaking. For end-users and policymakers, data at both spatial and temporal scales finer than those at which the climate projections are generated are highly useful but it becomes important to understand the limitations and uncertainties that come along before using them for their study which warrant detailed evaluations. This might also have implications over different regions (with different standards of available observations) when the end-user might need to investigate the data in greater detail, especially at daily scales. For end-users, it is also recommended to use a larger ensemble of models that could provide a higher confidence on climate projections while choosing specific models that perform well over their region.

References

Adam JC, Lettenmaier DP (2003) Adjustment of global gridded precipitation for systematic bias. J Geophys Res 108:1–14

Bao Y, Wen X (2017) Projection of China's near- and long-term climate in a new high-resolution daily downscaled dataset NEX-GDDP. J Meteorol Res. https://doi.org/10.1007/s13351-017-6106-6

Bosshard T, Carambia M, Goergen K, Kotlarski S, Krahe P, Zappa M, Schar C (2013) Quantifying uncertainty sources in an ensemble of hydrological climate-impact projections. Water Resour Res 49:1523–1536. https://doi.org/10.1029/2011WR011533

Chotamonsak C, Salathé EP Jr, Kreasuwan J, Chantara S, Siriwitayakorn K (2011) Projected climate change over Southeast Asia simulated using a WRF regional climate model. Atmos Sci Let 12:213–219

Christensen JH, Carter TR, Rummukainen M, Amanatidis G (2006) Evaluating the performance and utility of regional climate models: the PRUDENCE project. Clim Chang 81(1):1–6

Dufresne et al (2013) Climate change projections using the IPSL-CM5 Earth System Model: from CMIP3 to CMIP5. Clim Dyn 40:2123–2165

Giorgetta et al (2013) Climate and carbon cycle changes from 1850 to 2100 in MPI-ESM simulations for the Coupled Model Intercomparison Project Phase 5. J Adv Model Earth Syst 5:572–597

Giorgi F (1990) Simulations of regional climate using a limited area model nested in a general circulation model. J Clim 3(9):941–963

Harris I, Jones PD, Osborn TJ, Lister DH (2014) Updated high-resolution grids of monthly climatic observations - the CRU TS310 dataset. Int. J Clim 25(3):623–642

Hewitson BC, Crane RG (2006) Consensus between GCM climate change projections with empirical downscaling: precipitation downscaling over South Africa. Int J Climatol 26(10):1315–1337

Hirsch RM, Slack JR, Smith RA (1982) Techniques of trend analysis for monthly water quality data. Water Resour Res 18(1):107–121. https://doi.org/10.1029/WR018i001p00107

Ho TMH, Phan VT, Le NQ, Nguyen QT (2011) Extreme climatic events over Vietnam from observational data and RegCM3 projections. Clim Res 49:87–100

Hur J, Raghavan SV, Nguyen NS, Liong SY (2017) Are satellite products good proxies for gauge precipitation over Singapore? Theor Appl Climatol. https://doi.org/10.1007/s00704-017-2132-7

IPCC (2007) Climate Change 2007: The Physical Science Basis. In: Solomon S, Qin D, Manning M, Chen Z, Marquis M, Averyt KB, Tignor M, Miller HL (eds) Contribution of Working Group I to the Fourth Assessment Report of the Intergovernmental Panel on Climate Change. Cambridge University Press, Cambridge

Jacob D, Petersen J, Eggert B et al (2014) EURO-CORDEX: new high-resolution climate change projections for European impact research. Reg Environ Change 14(2):563–578

Kendall MG (1975) Rank correlation methods, 4th edn. Charles Griffin, London

Mann HB (1945) Non-parametric tests against trend. Econometrica 13:245–259. https://doi.org/10.2307/1907187

Maraun D, Widmann M (2018) Statistical downscaling and bias correction for climate research. Cambridge University Press. https://doi.org/10.1017/9781107588783

Maurer EP, Adam JC, Wood AW (2009) Climate model based consensus on the hydrologic impacts of climate change to the Rio Lempa basin of Central America. Hydrol Earth Syst Sci 13:183–194

SEACAM (2014) A regional climate modelling experiment for Southeast Asia, technical report initiated by the Centre for Climate Research Singapore of the Meteorological Service Singapore (CCRS-MSS) in collaboration with the Met Office Hadley Centre (MOHC), UK

Sheffield J, Goteti G, Wood EF (2006) Development of a 50-year high-resolution global dataset of meteorological forcings for land surface modeling. J Clim 19:3088–3111

Shongwe ME, Lennard C, Liebmann B, Kalognomou E-A, Ntsangwane L, Pinto I (2015) An evaluation of CORDEX regional climate models in simulating precipitation over Southern Africa. Atmos Sci Lett 16(3): 199–207

Siew JH, Tangang FT, Juneng L (2014) Evaluation of CMIP5 coupled atmosphere-ocean general circulation models and projections of the Southeast Asian winter monsoon in the 21st century. Int J Clim 34:287–2884

Taylor KE (2001) Summarizing multiple aspects of model performance in a single diagram. J Geophys Res: Atmos 106(D7):7183–7192

Thrasher B, Maurer EP, McKellar C, Duffy PB (2012) Technical note: bias correcting climate model simulated daily temperature extremes with quantile mapping. Hydrol Earth Syst Sci 16(9):3309–3314

Trzaska S, Schnarr E (2014) A review for downscaling methods for climate change projections. USAID report by the Center for International Earth Science Information Network (CIESIN), 45 pp

Voldorie et al (2013) The CNRM-CM5.1 global climate model: description and basic evaluation. Clim Dyn 40: 2091–2121

Watanabe et al (2010) Improved climate simulation by MIROC5: mean states, variability, and climate sensitivity. J Clim 23:6312–6335

Yukimoto et al (2012) A new global climate model of the Meteorological Research Institute: MRI-CGCM3–model description and basic performance. J Meteorol Soc Jpn 90A:23–64